# Decolorization of Reactive Blue 220 aqueous solution using fungal synthesized $Co_3O_4$ nanoparticles

Riya Sidhikku Kandath Valappil, Ajuy Sundar Vijayanandan and Raj Mohan Balakrishnan

## ABSTRACT

In this work, the photocatalytic activity of the biosynthesized cobalt oxide ($Co_3O_4$) nanoparticle (NP) is investigated using a textile dye Reactive Blue 220 (RB220) and decolorization % was monitored using UV–Vis spectrophotometer. The photocatalytic activity has been observed maximum at alkaline pH of 9, NP dosage of 250 mg/L, and reaction time of 270 min. In the presence of UV light irradiation, a maximum dye concentration of 10 mg/L was treated effectively using 150 mg/L NP, and 67% decolorization was achieved. Reaction kinetics has been analyzed, and the reaction followed the pseudo kinetics model with an activation energy of $-484$ kJ mol$^{-1}$.

**Key words** | $Co_3O_4$ nanoparticles, decolorization, kinetics, photocatalysis, RB220

**Riya Sidhikku Kandath Valappil**
**Ajuy Sundar Vijayanandan**
**Raj Mohan Balakrishnan** (corresponding author)
Department of Chemical Engineering,
National Institute of Technology Karnataka,
Surathkal, Mangaluru 575025, Karnataka,
India
E-mail: *rajmohanbala@gmail.com*

## INTRODUCTION

Energy demand, which had been outstripping supplies in the last few years, has led to an enormous increase in price. While it may be necessary to learn how to manage with much less energy, the highest priority should be given to developing energy solutions that can provide plentiful energy in the decades to come. Thus, the need of the hour is to find alternative sources of energy that are clean, cheap, and abundant, with minimal environmental impacts in energy extraction, conversion, and energy consumption. Energy harvesting and storage have nowadays attracted tremendous research efforts due to the rapid consumption of fossil fuels. While solar energy is abundant, it represents a tiny fraction of the world's current energy mix. But this is changing rapidly and is being driven by global action to improve energy access, and supply security, and to mitigate climate change (Faizal *et al.* 2015). Semiconductor nanoparticles (NPs) offer an attractive choice for increasing the efficiency of energy harvesting. Conversion of light energy into chemical energy through photocatalysts is a way of utilizing light and the same has been used for the treatment of industrial wastewaters like textile, paper, etc., contain non-biodegradable dyes in trace quantities (Sharma *et al.* 2012). Synthetic dyes are used in textile and paper industries due to the broad color spectrum (Kushwaha *et al.* 2018). Textile industries generate deep-colored effluents containing carcinogenic dye materials, causing allergic dermatitis, skin irritation, and mutation in humans, plants, and animals (Moon *et al.* 2018; Karthikeyan *et al.* 2019). These compounds also avert the sunlight to enter plants and animals in the water, thereby annihilating photosynthetically active radiation in the ecosystem (Saleh 2018). To provide a clean aquatic environment, photocatalytic degradation has been used to remove harmful recalcitrant compounds by mineralization (Manimozhi *et al.* 2018). Though methods to remove dye include coagulation, membrane separation, flocculation, chemical oxidation, photochemical degradation, anaerobic biological degradation, and electrochemical oxidation have been employed, they exhibit low removal efficiency, require stern operating conditions, and high energy demand (Moon *et al.* 2018; Xu *et al.* 2018). Due to the chemical stability of most of the dyes, advanced oxidation processes have been employed for the degradation of dyes into environmentally benign products,

doi: 10.2166/aqua.2019.086

which is based on the formation of hydroxyl radicals in the solution for mineralization of dyes through the usage of NPs (Kushwaha *et al.* 2018). For azo dyes, biological decolorization is not a quite useful technique (Saleh 2018). Peculiar optical properties and small size render semiconductor NPs as interesting candidates for applications in optoelectronics, catalysts, and fluorescence spectroscopy (Sharma *et al.* 2012). Metal oxides are impressive to detoxify organic pollutants (Manimozhi *et al.* 2018), and metal oxide photocatalysis has the potential to transform organic dyes into $CO_2$, $H_2O$, and other non-toxic compounds (Saleh 2018). Also, photocatalysis in the presence of NPs offers a great solution for the elimination of pollutants from the environment. The advantage of the process is that only NPs and dye are the two components added to the reaction mixture without the involvement of harsh chemicals and conditions (Saleh 2018). Thus, it is one of the novel ways to treat water pollution in a fast, economical, and eco-friendly manner.

Reactive Blue 220 (RB220) is vinyl sulfone azo dye mainly used in textile industries and more than 50% of cotton is dyed with reactive dyes only (Niebisch *et al.* 2010). RB220 has been degraded in only two cases when nanomaterials are used (Mahmoodi *et al.* 2006; Khanna & Shetty 2014). Tricobalt tetroxide or cobalt oxide ($Co_3O_4$) NPs are one of the emerging and promising materials for efficient degradation of various effluents. Most of the studies revolving around cobalt oxide NPs for dye degradation were observed for the treatment of methylene blue (MB) dye (Farhadi *et al.* 2016; Bazgir & Farhadi 2017; Mathew & Shetty 2017; Nassar *et al.* 2017; Vennela *et al.* 2019). Very few studies have been carried out on the potential of cobalt oxide NPs for other dyes namely, rhodamine B (32% decolorization), and direct red 80 (78% decolorization) (Dhas *et al.* 2015), methyl orange, and rhodamine B (Abbasi *et al.* 2018), eosine blue (Koli *et al.* 2018), and methyl orange (Saeed *et al.* 2019). In this work, the efficiency of cobalt oxide NPs synthesized through endophytic fungus was utilized for the photocatalytic decolorization of RB220 dye through the electron transfer process.

Though biological methods for synthesizing NPs have already been explored in earlier studies, the involvement of endophytic fungus for the synthesis of $Co_3O_4$ NPs has not been reported (Kumar *et al.* 2008; Shim *et al.* 2011; Diallo *et al.* 2015; Bibi *et al.* 2017; Khalil *et al.* 2017; Saeed *et al.* 2019). $Co_3O_4$ NPs have been mainly synthesized by the bacterial method and plant extracts in biological methods of synthesis. $Co_3O_4$ NPs prepared from sunflower extract have been used for the degradation of methyl orange (Saeed *et al.* 2019). $Co_3O_4$ NPs synthesized from *Punica granatum* have been used to degrade Remazol Brilliant Orange dye (Bibi *et al.* 2017). In the current study, the endophytic fungus was isolated from a native medicinal plant, *Nothapodytes foetida* and used for the first time to synthesize $Co_3O_4$ NPs. Further, for the first time, the biologically synthesized $Co_3O_4$ NPs are being utilized for the decolorization of RB220 dye. Hence, the current work can be considered as a novel work for engaging biologically synthesized $Co_3O_4$ NPs in the decolorization of RB220.

The photocatalytic potential of $Co_3O_4$ NP is being tested using the dye RB220 at different time, pH, dye concentration (mg/L), and NP concentration (mg/L). Meanwhile, the decolorization efficiency of $Co_3O_4$ NP has been determined, and a mechanism and kinetics of the RB220 decolorization have been elucidated.

## EXPERIMENTAL

### $Co_3O_4$ NP synthesis

The synthesis of cobalt oxide NPs using endophytic fungus, *Aspergillus nidulans* isolated from the plant *Nothapodytes foetida* as the reducing agent, and cobalt (II) acetylacetonate as precursor compound was reported by Vijayanandan & Balakrishnan (2018). The scheme has been depicted in Figure 1(a).

### Materials

To assess the decolorization by cobalt oxide NPs, and since textile effluent contains RB220 dye, RB220 (Indian Fine Chemicals Pvt Ltd, Bengaluru, India) solution has been used in the present study. The structure of RB220 has been given in Figure 1(b). Stock solutions of the dye were formulated by dissolving dyestuff powder in distilled water to a concentration of 0.005% (w/v). Different concentration of the dye was prepared by taking appropriate volumes of the stock solution, and the pH of the dye solution was adjusted to the desired value using 0.1 M NaOH or 0.1 M HCl.

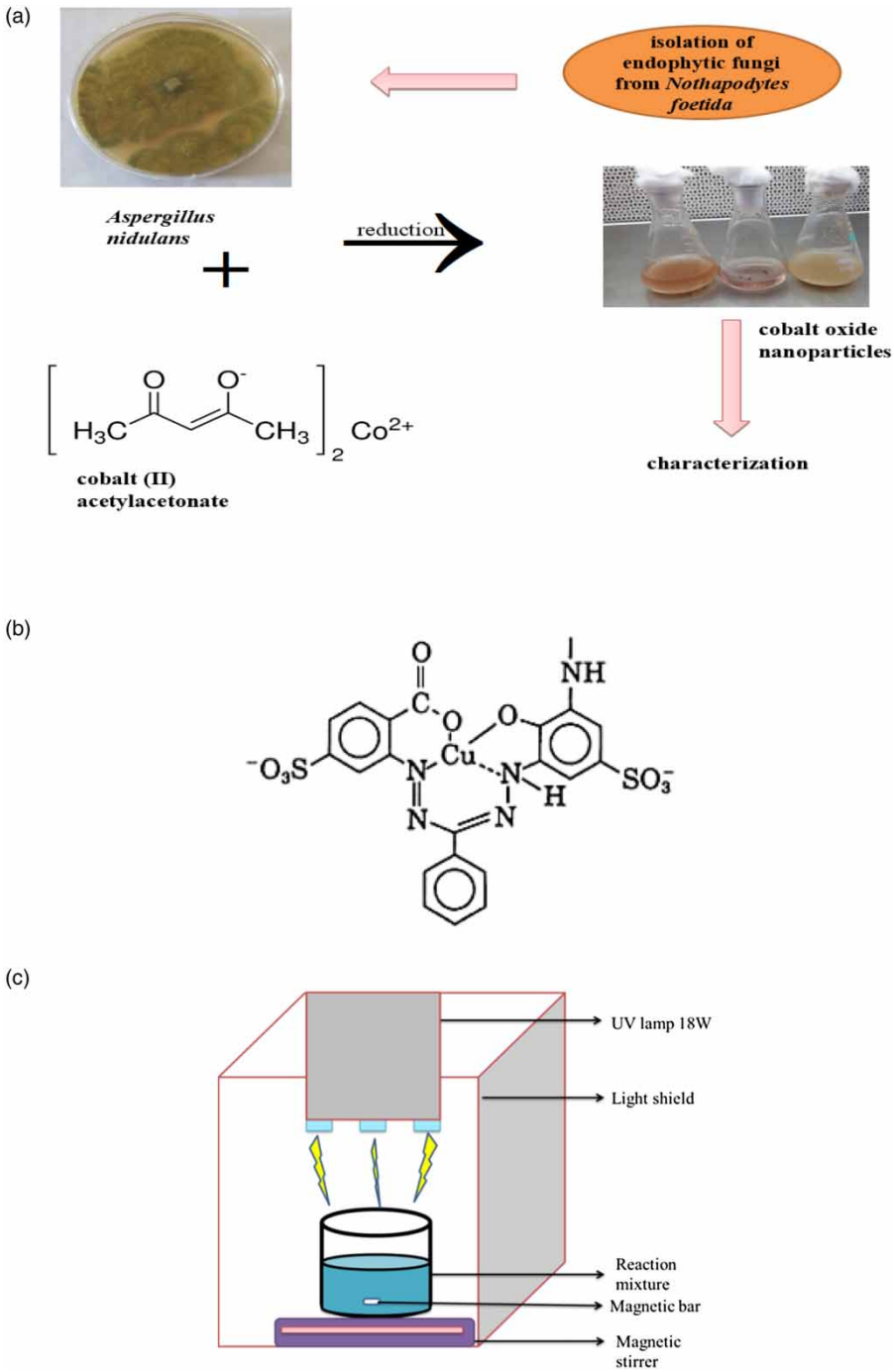


**Figure 1** | (a) Synthesis of cobalt oxide nanoparticles (Vijayanandan & Balakrishnan 2018), (b) structure of RB220 dye (Boduroğlu *et al.* 2014), and (c) experimental set-up for RB220 degradation.

## Method for photocatalytic degradation of RB220

Photocatalytic activity of $Co_3O_4$ NP was examined by the degradation of RB220 under UV light in the range of 315–400 nm as regards to time. 20 mL of RB220 dye was taken from the stock solution, and 3 mg of $Co_3O_4$ NP was added to the dye solution. Since the natural pH of the dye solution was 6.5–7 and to attain an adsorption–desorption

equilibrium, the reaction mixture was stirred in the dark for 30 min on a magnetic stirrer (KMS 450, Kadavil Electro Mechanical Industries, Kerala, India) before exposing to the UV light. Figure 1(c) shows the schematic of the experimental set-up which consists of an aluminum chamber equipped with three UV lamps as an irradiation source (Philips TL-D 18 W, India). A 250 mL borosilicate glass beaker was used as the reactor, which was placed inside the closed aluminum chamber, and the reaction mixture was magnetically stirred constantly at room temperature. The aliquots of the sample were periodically withdrawn, centrifuged at 5,000 rpm for 10 min before measuring the absorbance for removing nanocatalysts, and the progress of the reaction was tracked by measuring absorbance at 609 nm of clear supernatants using UV–Vis spectrophotometer (Shimadzu UV-1800, Labomed, USA).

Dye decolorization efficiency of $Co_3O_4$ NP was estimated using the following Equation (1):

$$\text{Decolorization efficiency} = \left[\frac{A_i - A_t}{A_i}\right] \times 100\% \quad (1)$$

where $A_i$ is the initial absorbance of the dye, and $A_t$ is the absorbance of the dye at any time interval (Forootanfar *et al.* 2012).

## Effect of parameters and measurement of chemical oxygen demand

The optimum time for dye decolorization was determined by irradiating the samples with UV light and measuring their absorbances at 609 nm for every 15 min up to 5 h. The pH of the dye solution was adjusted to 7 by adding 0.1 M NaOH and 0.1 M HCl, keeping both the concentration of the dye and NPs constant at 20 mg/L and 150 mg/L, respectively. The influence of dye concentration on photocatalytic decolorization was investigated for a range between 10 mg/L and 50 mg/L for the optimum pH, contact time, and concentration of the NP obtained from the previous experiments. The impact of NP concentration was explored by adding 150 mg/L, 250 mg/L, 350 mg/L, 450 mg/L, and 550 mg/L concentrations of NPs to dye solution at optimized pH, the concentration of dye, and contact time. The chemical oxygen demand (COD) of the samples was determined at regular intervals using the dichromatic oxidation method, which involves standard titration procedure taking distilled water as blank.

## Kinetics

The kinetics model of decolorization of dye is a pseudo-first-order rate equation represented by Equation (2)

$$\frac{dC_t}{dt} = -k_1 C \quad (2)$$

where $k_1$ is the first-order rate constant, $C_t$ is the concentration of the dye at $t$ min, and $t$ is the reactive time.

When $t = 0$, $C_t$ is equal to $C_0$ and the Equation (2) becomes Equation (3) as follows:

$$C_t = C_0 e^{-k/t} \quad (3)$$

## Statistical analysis

Absorbance data obtained at two different pHs (7, 9), and NP concentrations (150 mg/L and 250 mg/L) were analyzed by one-way analysis of variance (ANOVA) test using a free online calculator to determine the effect of pH and NP concentration (Tables 1 and 2). Significance level ($\alpha$) was set at 0.05, and the statistical significance values ($p$-value) for different pH and NP concentrations were determined and compared. To find out whether the means between two

**Table 1** | Absorbance data at different pH for statistical analysis – one-way ANOVA

| S.No. | pH 7 | pH 9 |
|---|---|---|
| 1 | 0.079 | 0.052 |
| 2 | 0.077 | 0.053 |

**Table 2** | Absorbance data at nanoparticle concentration for statistical analysis – one-way ANOVA

| S.No. | 150 mg/L | 250 mg/L |
|---|---|---|
| 1 | 0.075 | 0.066 |
| 2 | 0.076 | 0.07 |

populations are statistically different, the ratio of variation between the sample means and variation within samples was also estimated (*F*-value).

## RESULTS AND DISCUSSIONS

### Effect of time

To establish an efficient photocatalyst, insight about the equilibrium time is needed as it is one of the most essential parameters. For this intent, the removal of RB220 was examined as a function of time (El-Gamal *et al.* 2015). From Figure 2(a), it is clear that the rate of decolorization increases with time. As a greater number of NPs bind to dye with a rise in contact time, there is a critical decrease in absorbance after 170 min of UV light irradiation, leading to constancy in removal efficiency. Increase in treatment span hints at more time access for the reaction of dye decolorization (Kale & Kane 2016). Further, it increases electron–hole formation, preventing recombination, which leads to higher production of hydroxyl radicals (Sari *et al.* 2017).

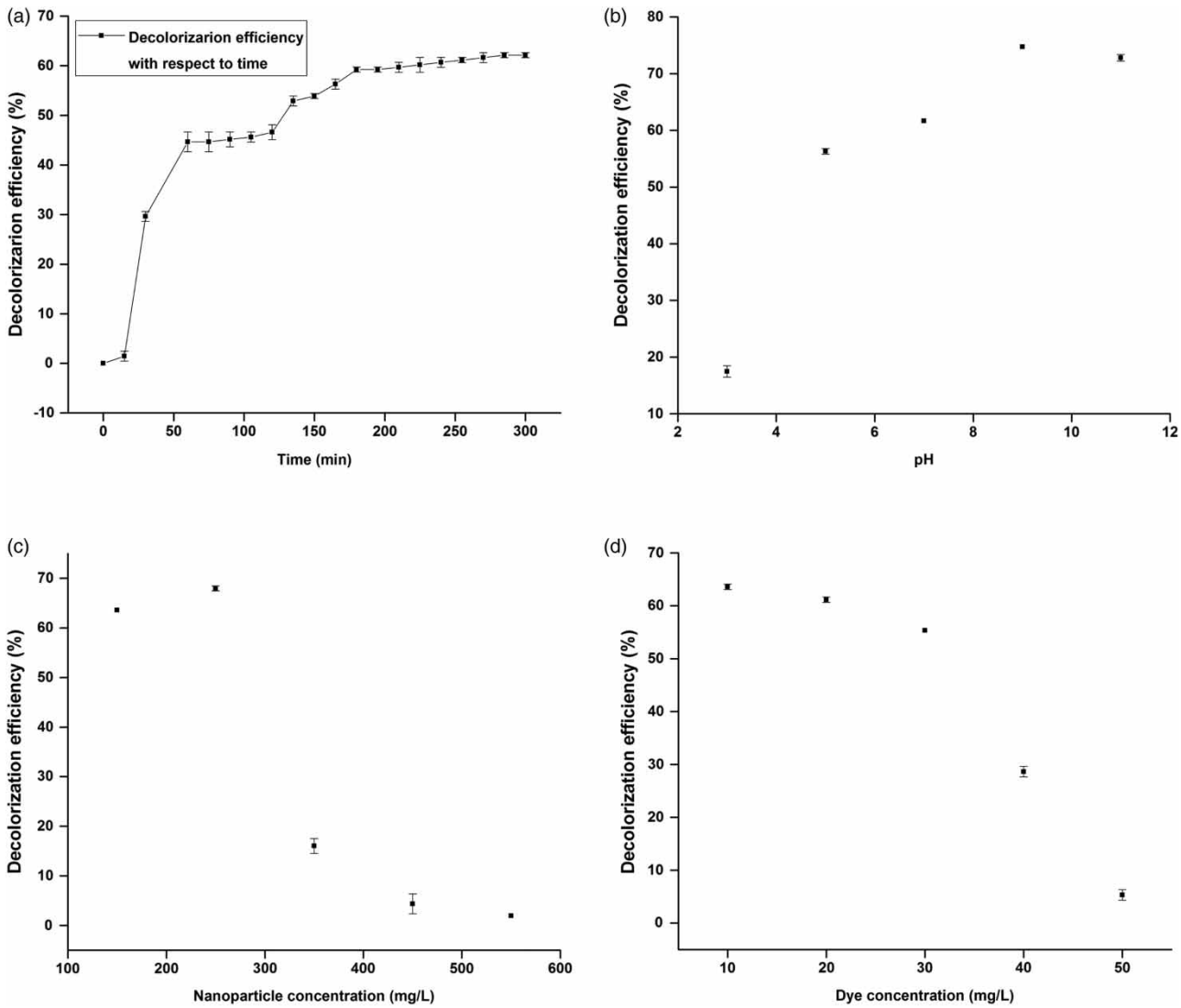


**Figure 2** | Effect of parameters: (a) Decolorization efficiency of RB220 dye with respect to time. (b) Decolorization efficiency of $Co_3O_4$ nanoparticles with respect to pH (dye concentration = 20 mg/L, nanoparticle dosage = 150 mg/L). (c) Decolorization efficiency of nanoparticles with respect to $Co_3O_4$ nanoparticles' concentration (dye concentration = 10 mg/L, pH = 9). (d) Decolorization efficiency of nanoparticles with respect to dye concentration ($Co_3O_4$ concentration = 150 mg/L, pH = 9).

Maximum decolorization was observed to be 62% at 270 min (Figure 2(a)). This might be due to the unavailability of active sites on NPs for adsorption of the dye or due to inadequate NPs for the dye to get adsorbed (El-Gamal *et al.* 2015). Since the increase in decolorization efficiency is negligible after 270 min, the aforementioned is taken as the optimum time to carry out further experiments. The dye decolorization by $Co_3O_4$ NP was authenticated by a decrease in absorbance and visually detected by a gradual decrease in the intensity of the color of the dye solution (Deshmukh *et al.* 2018).

## Effect of pH

The pH of the solution can have a great influence on the adsorption of dyes on the NP surface and thus is a crucial factor in photocatalysis (Thu *et al.* 2016). The effect of the pH of the dye on the decolorization efficiency has been presented in Figure 2(b). PH regulates surface characteristics, the charge of organic molecules, and the size of NPs, thereby altering the adsorption of dye molecules on the surface of NPs (Azeez *et al.* 2018). From Figure 2(b), it is evident that the decolorization efficiency progressed with the rise in pH and attained 74% at pH 9. The removal efficiency was greater in the alkaline pH when compared to the acidic pH (Figure 2(b)). The electrostatic interaction is higher between dye molecules, and the surface of NPs at pH 9, paving the way to the highest degree of oxidation, causing enhancement in photocatalytic decolorization of dye molecules (Alshabanat & Al-Anazy 2018). The isoelectric point (IEP) of cobalt oxide semiconductors is relatively high at around 8 (Kittaka & Morimoto 1980; Elhag *et al.* 2015). Thus, the surface of NPs is positively charged in an acidic environment and negatively charged in alkaline solutions. At lower pH below the IEP, $H^+$ ions compete effectively with dye cations, causing a reduction in decolorization efficiency. Furthermore, a low pH associated with a positively charged surface cannot provide the hydroxyl group, which is needed for hydroxyl radical formation. At higher pH above IEP, the surface of NP gets negatively charged, which enhances the adsorption of positively charged dye cations. However, the decolorization of dye molecules is hindered when the pH value is so high (pH > 9), because the hydroxyl ions compete with dye molecules in adsorption on the surface of NPs (Shamsipur & Rajabi 2014). Further increase in pH may augment the electron–hole recombination rate, abating the photocatalytic activity (Mohamed *et al.* 2012).

## Effect of dye concentration

It is observed from Figure 2(c) that decolorization efficiency diminishes with an escalation in dye concentration. The maximum removal of dye is 10 mg/L concentration with 150 mg/L concentration of NPs. The observed decrease in decolorization % with increasing dye concentration can be due to the following reasons: (i) more dye molecules interacted over the surface of the NPs as the initial concentration of dye increased, which reduced the generation of hydroxyl ions at the surface of the NP as the active sites have been occupied by dye molecules; (ii) An increment in the light absorbed by the dye molecules may lead to a decrease in the number of photons that reach the NP surface (Shamsipur & Rajabi 2014). The sites on the surface of NPs have saturated with time, leading to competitive adsorption of oxygen on the sites, thereby slowing down the generation of radicals. Another factor is contention for photogenerated holes between adsorbed molecules of water and RB220 molecules (Alshabanat & Al-Anazy 2018).

## Effect of $Co_3O_4$ NP dosage

As summarized in Figure 2(d), the decolorization of RB220 was found to rise with an increase in the NP concentration up to 250 mg/L for a fixed concentration of dye. The total active surface area and availability for binding increased with the enhancement in the NPs dosage. Strengthening the NPs concentration amplified to a higher number and density of NPs, which in turn caused photons to be absorbed, and hence, gain in the adsorption of dye molecules would happen. The dosage of NPs plays a key role in the efficiency of photocatalytic degradation of dyes. An increase in the NP concentration increases the number of active sites, which are charge carriers that engage in photoactivity leading to decolorization and degradation of the dye (Saleh 2018). Further,

there is more possibility of a catalyst for attacking chromophores in dye (Kale & Kane 2016). All of these cases have led to enrichment in the efficiency of decolorization. A further increase in the NP count beyond the optimum dosage decreases the photo-decolorization by some margin thanks to the overlapping of adsorption sites as a result of overcrowding and owing to a collision with ground state catalyst. The opacity of the suspensions also increases with the hike in the concentration of NPs which in turn accelerates the light scattering and resulted in a reduction in the penetration depth of the photons, and hence, only a lesser number of NPs were activated (El-Gamal *et al.* 2015). Besides, higher catalyst concentration increases the turbidity of the solution, preventing the path of irradiation to reach the sample (Mohamed *et al.* 2012). Maximum decolorization of 67% has been achieved at NP concentration of 250 mg/L. Thus, with an increase in NP concentration, decolorization efficiency also enhanced. However, this relation does not extend linearly as it reached a saturation point leading to hindrance for the entire decolorization of dye. The results prove that even a smaller quantity of NPs is adequate for decolorization with fair results. In two cases only, NPs have been used to decolorize RB220 dye (Mahmoodi *et al.* 2006; Khanna & Shetty 2014). Mahmoodi *et al.* 2006 used an immobilized $TiO_2$ photocatalytic reactor with the addition of an $H_2O_2$ concentration of 450 mg/L with RB220 concentration 50 mg/L at pH 6 having irradiation time of 90 min, yet decolorization efficiency datum is unavailable. Ag@$TiO_2$ core–shell NPs were used by Khanna & Shetty (2014), as noble metal Ag is a core, and semiconductor dioxide $TiO_2$ is used as a shell. Decolorization efficiency of RB220 dye was achieved to be 98.9%, when RB220 of 50 mg/L and NP dosage of 1 g/L at pH 3 were irradiated for 240 min in UV light. Thus, a single type of NP in beakers has not been used for RB220 degradation, indicating this current study is a prime one.

## COD analysis

COD values provide information about the toxicity of photocatalyzed solutions (Ertugay & Acar 2017), and since the absorbance values in spectrophotometry cannot be related to the reduction of COD, it is indispensable to know the imprint of NPs on the COD value of dye solution (Kale & Kane 2016). In Figure 3, as time proceeds, COD reduces in the supernatant as more and more dye gets accumulated over the NP surface (Nezamzadeh-Ejhieh & Shams-Ghahfarokhi 2013). This has led to the inference of NP resulting in the decolorization of dye, ultimately decrease in the value of COD, attesting the degradation of RB220 (Kale & Kane 2016).

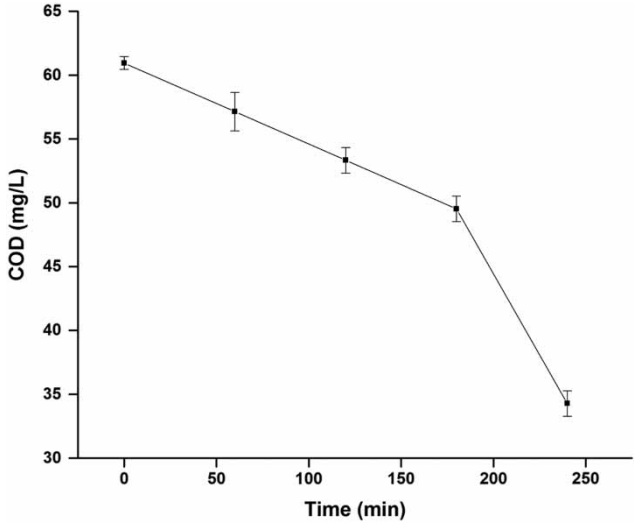


**Figure 3** | COD analysis of the reaction mixture with respect to time.

## Mechanism of dye removal

Photocatalytic dye degradation banks on the transfer of electrons between donor and acceptor causing an electron relay system (Nakkala *et al.* 2018). The decrease in the absorbance is related to the electron relay effect (Joshi *et al.* 2018). When cobalt oxide NPs are irradiated and bombarded against photons from the light source with energy ($h\nu$) energy greater than or equal to its bandgap (3.4 eV) (Vijayanandan & Balakrishnan 2018), the electrons get excited and move to the conduction band from valence band, leaving out a hole in the valence band. These electrons react with oxygen atoms to give superoxide radical anion $O_2^-$ and holes which undergo oxidation to react with water to give hydroxyl ions and eventually hydroxyl radicals. These reactions together subsequently yield highly oxidant species like hydroperoxyl radicals, thereby yielding peroxide. Thus, the

peroxide radicals attack and break down the bonds of the azo group in the dye and produce lower molecular weight compounds like formate, acetate, glyoxylate, and oxalate (Mahmoodi *et al.* 2006). Lastly, the intermediate compounds have been further mineralized into $CO_2$ and $H_2O$, leading to the decolorization of the dye (Norzaee *et al.* 2017). The blue color of the dye dimmed and turned into colorless during the process (Fairuzi *et al.* 2018). This phenomenon is attributed to the Surface Plasmon Resonance effect (oscillation of charge density propagating at the interface), in which excited surface electrons react with dissolved molecules, producing hydroxyl molecules (Selvam & Sivakumar 2015; Kumari *et al.* 2016). The above mechanism of degradation of the dye RB220 has been depicted in Figure 4.

## Kinetics

Kinetics curve for the pseudo-first-order reaction representing the reaction between NPs and dye was drawn. The integrated rate law of the Equation (4) is

$$[A] = [A]_0 e^{-kt} \tag{4}$$

The rate constant for the reaction obtained from the slope (Figure 5(a)) is 0.0029 $s^{-1}$ and the coefficient of determination ($R^2$) is 0.823. Activation energy obtained from the Arrhenius plot (Figure 5(b)) is equal to −484 kJ $mol^{-1}$, and the pre-exponential factor is found to be −190.6.

The reaction kinetics has been noticeable from the color change of the reaction as evident from Figure 5(a) and 5(b).

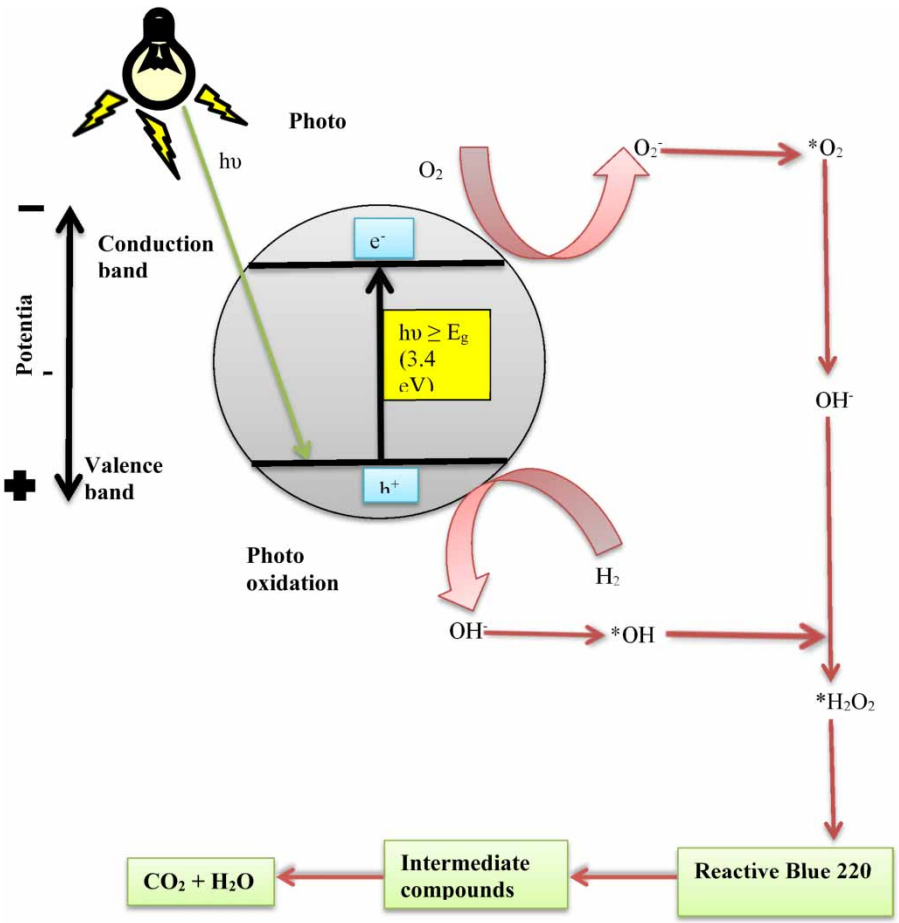


**Figure 4** | Mechanism of RB220 degradation by hydroxyl radicals.

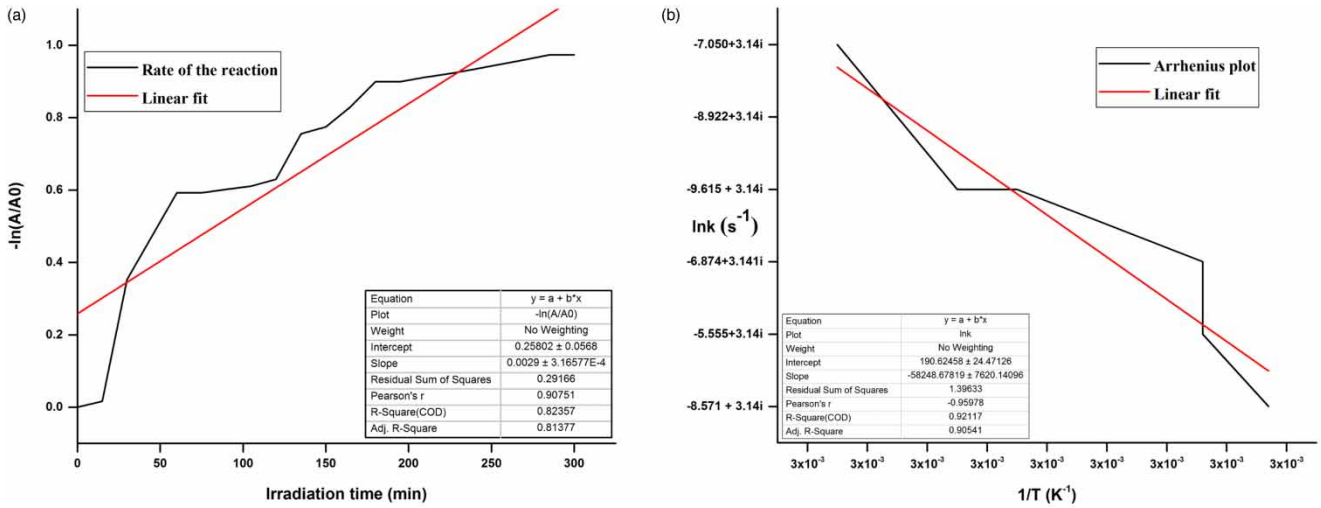


**Figure 5** | Kinetics of the study: (a) pseudo-first-order decay curve, (b) Arrhenius plot of reaction.

Before the reaction, the solution was deep blue. But after the reaction with NPs, the solution became pale blue due to the decolorization phenomenon.

## Statistical analysis

Tables 3 and 4 show ANOVA results, from which *p*-value and *F*-value were deduced. The *p*-value (0.0019) for the solution at different pH (7, 9) was lower than the significance level indicating that the mean absorbance values at different pH were not equal, and hence, the null hypothesis was rejected. *F*-value (530.81) was found to be greater than 1, which confirms the rejection of the null hypothesis. However, for different NP concentrations (mg/L) (150, 250), the *p*-value (0.0667) is significant, accepting the null hypothesis, though *F*-value (13.50) cannot confirm the same.

**Table 3** | ANOVA for absorbance at pH (7, 9)

| S.No. | pH | Mean | Std. dev. | Std. error |
|---|---|---|---|---|
| 1 | 7 | 0.078 | 0.0014 | 0.001 |
| 2 | 9 | 0.0525 | 0.007 | 0.0005 |

**Table 4** | ANOVA for absorbance at nanoparticle concentration (mg/L) (150, 250)

| S.No. | Nanoparticle concentration (mg/L) | Mean | Std. dev. | Std. error |
|---|---|---|---|---|
| 1 | 150 | 0.0755 | 0.0007 | 0.0005 |
| 2 | 250 | 0.068 | 0.0028 | 0.002 |

## PRACTICAL APPLICATION AND FUTURE RESEARCH PERSPECTIVES

Increase in the textile industries has led to an increase in the utilization of the dyes. Synthetic dyes cause pollution if discharged directly into the environment without treating the effluent. Most of the dyes are resistant to biological and physical treatment methods. $Co_3O_4$ NPs can be used as an efficient cure for a dye solution as they behave as a photocatalytic agent. The NPs can be used to treat wastewater containing commercial RB220 discharged from cotton industries. They can detoxify pollutants and reintroduce them into the nutrient cycle, thereby reducing the amount of sludge formed. They can also be employed in leather and furniture industries where a large number of synthetic dyes are used. RB220 is a textile dye, and photocatalysis by NPs is a simple electron transfer process, using light energy which can be converted into photocatalysts, which can be used for degradation of dyes in wastewater. By scaling up this process, the content of RB220 can be photo detoxified, and effluent can be decolorized. Reactor studies were performed in 5 L immobilized $TiO_2$ photocatalytic reactor for the degradation of RB220 in a batch mode (Mahmoodi *et al.* 2006). Further, the feasibility of scaling-up depends on

mass transfer, hydromechanics, operator-variability, mixing, and avoiding gradients. Thus, the process brings out the way for ecological health and environmental bioremediation. It is a widely accepted choice for environmental purification. So, the scheme has the potential to be a feasible solution for wastewater treatment. This work offers a sustainable solution using a promising strategy to mollify water pollution problems principally for developing countries, which experience dye effluents, especially when the financial budget is a constraint.

However, there are some limitations, which need to be rectified to establish a superior photocatalysis system. Biosynthesized $Co_3O_4$ NPs should be checked for photocatalytic ability in other azo dyes, as there will not be an effluent that contains only RB220 dye. Practically, there will be a mixture of dyes in the effluent generated by textile industries, and the impact of mixture on the efficiency of NPs is unknown. So, the photocatalytic potential of $Co_3O_4$ NPs should be checked for all other dyes in the effluent, before it is implemented for dye degradation in textile industries. Also, there is a doubt about $Co_3O_4$ NPs being non-specific to dyes present in the wastewater. There is a need to find a solution for the complete elimination of dyes in the effluent, so that water can be recycled and reused. Bazgir & Farhadi (2017) checked the reusability of $Co_3O_4$ NPs for 4 runs in the degradation of MB and a slight decline in activity was observed. Koli *et al.* (2018) checked the reusability for 4 runs for the degradation of eosine blue dye and found a decrease in activity. In addition, whether $Co_3O_4$ NPs will provide the same efficiency in the subsequent cycles when the same particles are washed and reused for treatment. So, the reusability of nanocatalysts has to be checked. Another problem is the durability of the NP system, and after scaling up, whether the dyebath can withstand a system continuously having $Co_3O_4$ NPs. The NPs can be attempted to degrade environmental pollutants like recalcitrant molecules and plastics. They can be utilized to treat oil spills. Additionally, they can also be tried to decontaminate polluted groundwater. Since factorial ANOVA involves more than two factors, it can be recommended as a future study in statistical analysis with the inclusion of different pH and NP concentrations.

## CONCLUSION

Decolorization of textile dye RB220 using biosynthesized $Co_3O_4$ NPs has been evaluated in this current study. A maximum dye concentration of 10 mg/L of RB220 was decolorized effectively using 150 mg/L concentration of $Co_3O_4$ NPs. The photocatalytic activity of the NPs has also led to the degradation of the dye as indicated by the reduction in COD of the dye solution. The decolorization rate follows the pseudo-first-order kinetics model. The decolorization efficiency for RB220 is found to be 67% which is significant in the case of the biologically synthesized $Co_3O_4$ NPs without any further modification and can be considered as a simple solution without the involvement of sophisticated instruments, toxic chemicals, and conditions.

## REFERENCES

Abbasi, A., Golsefidi, M. A., Beigi, M. M., Sadri, N. & Abroudi, M. 2018 Facile fabrication of $Co_3O_4$ nanostructures as an effective photocatalyst for degradation and removal of organic contaminants. *J. Nanostruct.* **8** (1), 89–96.

Alshabanat, M. N. & Al-Anazy, M. M. 2018 An experimental study of photocatalytic degradation of polymer using polymer nanocomposite films. *J. Chem.* **2018**, 8. Article 9651850.

Azeez, F., Al-Hetlani, E., Arafa, M., Abdelmonem, Y., Nazeer, A. A., Amin, M. O. & Madkour, M. 2018 The effect of surface charge on photocatalytic degradation of methylene blue dye using chargeable titania nanoparticles. *Sci. Rep.* **8** (1). Article 7104.

Bazgir, S. & Farhadi, S. 2017 Microwave-assisted rapid synthesis of $Co_3O_4$ nanorods from $CoC_2O_4 \cdot 2H_2O$ nanorods and its application in photocatalytic degradation of methylene blue under visible light irradiation. *Int. J. Nano Dimens.* **8** (4), 284–297.

Bibi, I., Nazar, N., Iqbal, M., Kamal, S., Nawaz, H., Nouren, S., Safa, Y., Jilani, K., Sultan, M., Ata, S., Rehman, F. & Abbas, M. 2017 Green synthesis of cobalt-oxide nanoparticle: characterization and photocatalytic activity. *Adv. Powder Technol.* **28** (9), 2035–2043.

Boduroğlu, G., Kılıç, N. K. & Dönmez, G. 2014 Bioremoval of reactive blue 220 by *Gonium* sp *Biomass*. *Environ. Technol.* **35** (19), 2410–2415.

Deshmukh, K. K., Hase, G. J., Gaje, T. R., Phatangare, N. D., Shilpa, G. & Ashwini, V. 2018 Titanium oxide nanoparticles and degradation of dye by nanoparticles. *Int. J. Mater. Sci.* **13** (1), 23–30.

Dhas, C. R., Venkatesh, R., Jothivenkatachalam, K., Nithya, A., Benjamin, B. S., Raj, A. M. E., Jeyadheepan, K. &

Sanjeeviraja, C. 2015 Visible light driven photocatalytic degradation of rhodamine B and direct red using cobalt oxide nanoparticles. *Ceram. Int.* **41** (8), 9301–9313.

Diallo, A., Beye, A. C., Doyle, T. B., Park, E. & Maaza, M. 2015 Green synthesis of $Co_3O_4$ nanoparticles via *Aspalathus linearis*: physical properties. *Green Chem. Lett. Rev.* **8** (3–4), 30–36.

El-Gamal, S. M. A., Amin, M. S. & Ahmed, M. A. 2015 Removal of methyl orange and bromophenol blue dyes from aqueous solution using Sorel's cement nanoparticles. *J. Environ. Chem. Eng.* **3** (3), 1702–1712.

Elhag, S., Ibupoto, Z. H., Nour, O. & Willander, M. 2015 Synthesis of $Co_3O_4$ cotton-like nanostructures for cholesterol biosensor. *Materials (Basel)* **8** (1), 149–161.

Ertugay, N. & Acar, F. N. 2017 Removal of COD and color from Direct Blue 71 azo dye wastewater by Fenton's oxidation: kinetic study. *Arabian. J. Chem.* **10** (1), S1158–S1163.

Fairuzi, A. A., Bonnia, N. N., Akhir, R. M., Abrani, M. A. & Akil, H. M. 2018 Degradation of methylene blue using silver nanoparticles synthesized from *Imperata cylindrica* aqueous extract. *IOP Conf. Ser. Earth Environ. Sci.* **105**. Article 012018.

Faizal, M., Saidur, R., Mekhilef, S., Hepbasli, A. & Mahbubul, I. M. 2015 Energy, economic and environmental analysis of a flat-plate solar collector operated with $SiO_2$ nanofluid. *Clean Technol. Environ. Policy* **17**, 1457–1473.

Farhadi, S., Javanmard, M. & Nadri, G. 2016 Characterization of cobalt oxide nanoparticles prepared by the thermal decomposition. *Acta. Chim. Slov.* **63** (2), 335–343.

Forootanfar, H., Moezzi, A., Aghaie-Khozani, M., Mahmoudjanlou, Y., Ameri, A., Niknejad, F. & Faramarzi, M. A. 2012 Synthetic dye decolorization by three sources of fungal laccase. *J. Environ. Health Sci. Eng.* **9** (1), 27.

Joshi, S. J., Geetha, S. J., Al-Mamari, S. & Al-Azkawi, A. 2018 Green synthesis of silver nanoparticles using pomegranate peel extracts and its application in photocatalytic degradation of methylene blue. *Nat. Pharm. Prod.* **13** (3), e67846.

Kale, R. D. & Kane, P. B. 2016 Color removal using nanoparticles. *Text. Cloth. Sust.* **2** (4). https://doi.org/10.1186/s40689-016-0015-4.

Karthikeyan, V., Ragunathan, R., Johney, J. & Kabesh, K. 2019 Green synthesis of silver nanoparticles and application in dye decolorization by *Pleurotus ostreatus* (MH591763). *J. Biosci. Biotechnol.* **8** (1), 80–86.

Khalil, N. M., Ovais, M., Ullah, M., Ali, M., Shinwari, Z. K. & Maaza, M. 2017 Physical properties, biological applications and biocompatibility studies on biosynthesized single-phase cobalt oxide nanoparticles ($Co_3O_4$) via *Sageretia thea* (Osbeck). *Arabian. J. Chem.* http://dx.doi.org/10.1016/j.arabjc.2017.07.004.

Khanna, A. & Shetty, V. 2014 Solar light induced photocatalytic degradation of reactive blue 220 (RB-220) dye with highly efficient Ag@$TiO_2$ core-shell nanoparticles: a comparison with UV photocatalysis. *Sol. Energy.* **99**, 67–76.

Kittaka, S. & Morimoto, T. 1980 Isoelectric point of metal oxides and binary metal oxides having spinel structure. *J. Colloid Interface Sci.* **75** (2), 398–403.

Koli, P. B., Kapadnis, K. H., Deshpande, U. G. & Patil, M. R. 2018 Fabrication and characterization of pure and modified $Co_3O_4$ nanocatalyst and their application for photocatalytic degradation of eosine blue dye: a comparative study. *J. Nanost. Chem.* **8**, 453–463.

Kumar, U., Shete, A., Harle, A. S., Kasyutich, O., Schwarzacher, W., Pundle, A. & Poddar, P. 2008 Extracellular bacterial synthesis of protein-functionalized ferromagnetic $Co_3O_4$ nanocrystals and imaging of self-organization of bacterial cells under stress after exposure to metal ions. *Chem. Mater.* **20** (4), 1484–1491.

Kumari, R. M., Thapa, N., Gupta, N., Kumar, A. & Nimesh, S. 2016 Antibacterial and photocatalytic degradation efficacy of silver nanoparticles biosynthesized using *Cordia dichotoma* leaf extract. *Adv. Nat. Sci.: Nanosci. Nanotechnol.* **7**. Article 045009.

Kushwaha, R., Garg, S., Bajpai, S. & Giri, A. S. 2018 Degradation of Nile blue sulphate dye onto iron oxide nanoparticles: kinetic study, identification of reaction intermediates and proposed mechanism pathways. *Asia. Pac. J. Chem. Eng.* **13** (3), e2200.

Mahmoodi, N. M., Arami, M., Limaee, N. Y. & Tabrizi, N. S. 2006 Kinetics of heterogeneous photocatalytic degradation of reactive dyes in an immobilized $TiO_2$ photocatalytic reactor. *J. Colloid Interface Sci.* **295** (1), 159–164.

Manimozhi, R., Kumar, D. R. & Prakash, A. P. G. 2018 Enhanced solar light driven photocatalytic degradation of organic dye using solution combustion synthesized $CeO_2$-ZnO nanocomposites. *J. Electron. Mater.* **47** (11), 6716–6721.

Mathew, J. & Shetty, N. 2017 Treatment of wastewater using synthesised photocatalyst cobalt oxide $Co_3O_4$. *Int. J. Civil Eng. Technol.* **8** (4), 1840–1844.

Mohamed, R. M., Mkhalid, I. A., Baeissa, E. S. & Al-Rayyani, M. A. 2012 Photocatalytic degradation of methylene blue by Fe/ZnO/$SiO_2$ nanoparticles under visible light. *J. Nanotechnol.* **2012**, 5. Article ID 329082.

Moon, S. A., Salunke, B. K., Saha, P., Deshmukh, A. R. & Kim, B. S. 2018 Comparison of dye degradation potential of biosynthesized copper oxide, manganese oxide and silver nanoparticles using *Kalopanax pictus* plant extract. *Korean J. Chem. Eng.* **35** (3), 702–708.

Nakkala, J. R., Mata, R., Raja, K., Chandra, V. K. & Sadras, S. R. 2018 Green synthesized silver nanoparticles: catalytic dye degradation, *in vitro* anticancer activity and *in vivo* toxicity in rats. *Mater. Sci. Eng. C* **91**, 372–381.

Nassar, M. Y., Aly, H. M., Abdelrahman, E. A. & Moustafa, M. E. 2017 Synthesis, characterization and biological activity of some novel Schiff bases and their Co(II) and Ni(II) complexes: a new route for $Co_3O_4$ and NiO nanoparticles for photocatalytic degradation of methylene blue dye. *J. Mol. Struct.* **1143**, 462–471.

Nezamzadeh-Ejhieh, A. & Shams-Ghahfarokhi, Z. 2013 Photodegradation of methyl green by nickel-dimethylglyoxime/ZSM-5 zeolite as a heterogeneous catalyst. *J. Chem.* **2013**, 1–11. Article 104093.

Niebisch, C. H., Malinowski, A. K., Schadeck, R., Mitchell, D. A., Kava-Cordeiro, V. & Paba, J. 2010 Decolorization and biodegradation of reactive blue 220 textile dye by *Lentinus crititus* extracellular extract. *J. Hazard Mater.* **180** (1–3), 316–322.

Norzaee, S., Djahed, B., Khaksefidi, R. & Mostafapour, F. K. 2017 Photocatalytic degradation of aniline in water using CuO nanoparticles. *J. Water Supply Res. Technol.* **66** (3), 178–185.

Saeed, M., Akram, N., Haq, A. U., Naqvi, S. A. R., Usman, M., Abbas, M. A., Abdeel, M. & Nisar, A. 2019 Green and eco-friendly synthesis of $Co_3O_4$ and Ag-$Co_3O_4$: characterization and photo-catalytic activity. *Green Process Synth.* **8**, 382–390.

Saleh, S. M. 2018 Metal oxide nanomaterials as photo-catalyst for dye degradation. *Res. Dev. Mater. Sci.* **9** (2), 1–8.

Sari, M. I., Agustina, T. E., Melwita, E. & Aprianti, T. 2017 Color and COD degradation in photocatalytic process of procion red by using TiO2 catalyst under solar irradiation. AIP Conf. Proc. 1903. Article 040017.

Selvam, G. K. & Sivakumar, K. 2015 Phycosynthesis of silver nanoparticles and photocatalytic degradation of methyl orange dye using silver (Ag) nanoparticles synthesized from *Hypnea musciformis* (Wulfen) J. V. Lamouroux. *Appl. Nanosci.* **5** (5), 617–622.

Shamsipur, M. & Rajabi, H. R. 2014 Study of photocatalytic activity of ZnS quantum dots as efficient nanoparticles for removal of methyl violet: effect of ferric ion doping. *Spectrochim. Acta A Mol. Biomol. Spectrosc.* **122**, 260–267.

Sharma, M., Jain, T., Singh, S. & Pandey, O. P. 2012 Photocatalytic degradation of organic dyes under UV-visible light using capped ZnS nanoparticles. *Sol. Energy* **86** (1), 626–633.

Shim, H., Jin, Y., Seo, S., Lee, S. & Kim, D. 2011 Highly reversible lithium storage in *Bacillus subtilis*-directed porous $Co_3O_4$ nanostructures. *ACS Nano* **5** (1), 443–449.

Thu, T. N. T., Thi, N. N., Quang, V. T., Hong, K. N., Minh, T. N. & Hoai, N. L. T. 2016 Synthesis, characterisation and effect of pH on degradation of dyes of copper-doped $TiO_2$. *J. Exp. Nanosci.* **11** (3), 226–238.

Vennela, A. B., Mangalaraj, D., Muthukumarasamy, N., Agilan, S. & Hemalatha, K. V. 2019 Structural and optical properties of $Co_3O_4$ nanoparticles prepared by sol-gel technique for photocatalytic application. *Int. J. Electrochem. Sci.* **14**, 3535–3552.

Vijayanandan, A. S. & Balakrishnan, R. M. 2018 Biosynthesis of cobalt oxide nanoparticles using endophytic fungus *Aspergillus nidulans*. *J. Environ. Manage.* **218**, 442–450.

Xu, J., Xu, D., Zhu, B., Cheng, B. & Jiang, C. 2018 Adsorptive removal of an anionic dye Congo red by flower-like hierarchial magnesium oxide (MgO)-graphene oxide composite microspheres. *Appl. Surf. Sci.* **435**, 1136–1142.

First received 14 June 2019; accepted in revised form 20 September 2019. Available online 13 November 2019